BJP British Journal of Pharmacology

DOI:10.1111/bph.12646
www.brjpharmacol.org

RESEARCH PAPER

PPARβ activation restores the high glucose-induced impairment of insulin signalling in endothelial cells

A M Quintela[1], R Jiménez[1], L Piqueras[2], M Gómez-Guzmán[1], J Haro[3], M J Zarzuelo[1], A Cogolludo[4], M J Sanz[2], M Toral[1], M Romero[1], F Pérez-Vizcaíno[4] and J Duarte[1]

[1]*Department of Pharmacology, University of Granada, 18071 Granada, Spain,* [2]*Department of Pharmacology, Faculty of Medicine, University of Valencia, Valencia, Spain,* [3]*Service of Gynecology, Clinic Hospital of Granada, Granada, Spain, and* [4]*Department of Pharmacology, School of Medicine, University Complutense of Madrid, IdISSC and Ciber Enfermedades Respiratorias (CIBERES), Madrid, Spain*

Correspondence
J Duarte, Department of Pharmacology, School of Pharmacy, University of Granada, 18071 Granada, Spain. E-mail: jmduarte@ugr.es

A M Quintela and R Jiménez: equal contributions as first authors.

Keywords
PPARβ; HUVECs; insulin signalling; reactive oxygen species

Received
18 September 2013
Revised
5 February 2014
Accepted
11 February 2014

BACKGROUND AND PURPOSE

PPARβ enhances insulin sensitivity in adipocytes and skeletal muscle cells, but its effects on insulin signalling in endothelial cells are not known. We analysed the effects of the PPARβ/δ (PPARβ) agonists, GW0742 and L165041, on impaired insulin signalling induced by high glucose in HUVECs and aortic and mesenteric arteries from diabetic rats.

EXPERIMENTAL APPROACH

Insulin-stimulated NO production, Akt-Ser^{473} and eNOS-Ser^{1177} phosphorylation, and reactive oxygen species (ROS) production were studied in HUVECs incubated in low- or high-glucose medium. Insulin-stimulated relaxations and protein phosphorylation in vessels from streptozotocin (STZ)-induced diabetic rats were also analysed.

KEY RESULTS

HUVECs incubated in high-glucose medium showed a significant reduction in insulin-stimulated production of NO. High glucose also reduced insulin-induced Akt-Ser^{473} and eNOS-Ser^{1177} phosphorylation, increased IRS-1-Ser^{636} and ERK1/2-Thr^{183}-Tyr^{185} phosphorylation and increased ROS production. The co-incubation with the PPARβ agonists GW0742 or L165041 prevented all these effects induced by high glucose. In turn, the effects induced by the agonists were suppressed when HUVEC were also incubated with the PPARβ antagonist GSK0660, the pyruvate dehydrogenase kinase (PDK)4 inhibitor dichloroacetate or after knockdown of both PPARβ and PDK4 with siRNA. The ERK1/2 inhibitor PD98059, ROS scavenger catalase, inhibitor of complex II thenoyltrifluoroacetone or uncoupler of oxidative phosphorylation, carbonyl cyanide m-chlorophenylhydrazone, also prevented glucose-induced insulin resistance. In STZ diabetic rats, oral GW0742 also improved insulin signalling and the impaired NO-mediated vascular relaxation.

CONCLUSION AND IMPLICATIONS

PPARβ activation *in vitro* and *in vivo* restores the endothelial function, preserving the insulin-Akt-eNOS pathway impaired by high glucose, at least in part, through PDK4 activation.

Abbreviations

AMPK, 5′-AMP-activated protein kinase; CCCP, carbonyl cyanide m-chlorophenylhydrazone; CPT-1, carnitine palmitoiltransferase-1; CM-H2DCFDA, 5-(and-6-)chloromethyl-2′-7′-dichlorodihydrofluorescein diacetate; DAF-2, diaminofluorescein-2; DCA, dichloroacetate; eNOS, endothelial nitric oxide synthase; IRS, insulin receptor substrate; L-NAME, N^{ω}-nitro-L-arginine methyl ester; mitoQ, mitoquinone; MnSOD, Mn-superoxide dismutase; Phe, phenylephrine; PDK4, pyruvate dehydrogenase kinase-4; ROS, reactive oxygen species; RT-PCR, reverse transcriptase-PCR; STZ, streptozotocin; TTFA, thenoyltrifluoroacetone

Introduction

Insulin resistance is characterized by the failure of insulin to suppress hepatic glucose production or stimulate glucose uptake by peripheral tissues, causing hyperglycaemia, hyperinsulinaemia and dyslipidaemia (Saltiel and Kahn, 2001; White, 2003; Taguchi and White, 2008). It is clinically important because it is closely associated with several diseases including type 2 diabetes, hypertension, dyslipidaemia and abnormalities in blood coagulation and fibrinolysis. One of the key vascular actions of insulin is to stimulate the production of the potent vasodilator NO from the endothelium (Vincent *et al.*, 2003) and, hence, insulin resistance is characterized by reduced insulin-induced NO release which may contribute to increased risk of vascular disease (Boden, 2011). The impaired insulin signalling in endothelial cells causes attenuation of insulin-induced capillary recruitment and insulin delivery, which, in turn, leads to a further reduction in glucose uptake by skeletal muscle (Kubota *et al.*, 2011).

The PPARs are members of the nuclear hormone receptor superfamily (see Alexander *et al.*, 2013). PPARs comprise three related receptors: PPARα, PPARβ/δ (PPARβ) and PPARγ. PPARs were initially believed to regulate genes involved only in lipid and glucose metabolism (Desvergne and Wahli, 1999; Lee *et al.*, 2003). PPARα is highly expressed in liver, where it controls peroxisomal and mitochondrial fatty acid catabolism, whereas PPARγ is abundant in adipose tissues, functioning as a key transcriptional factor for adipogenesis. The PPARα activators, such as the fibrates, are used for the treatment of hyperlipidaemia, whereas PPARγ agonists, such as the thiazolidinediones, are used to treat type 2 diabetes because they improve insulin action and decrease intracellular triglyceride accumulation in both liver and skeletal muscle (Miyazaki *et al.*, 2002; Tonelli *et al.*, 2004). PPARβ is expressed in most metabolically active tissues, controlling many genes involved in fatty acid metabolism and glucose homeostasis (Braissant *et al.*, 1996; Wang *et al.*, 2003). PPARβ has been shown to increase fat oxidation and reduce lipid accumulation in adipose tissue and in other tissues (Reilly and Lee, 2008). Furthermore, studies in rodents have shown that activation of PPARβ reduces body weight, increases metabolic rate and improves insulin sensitivity, through increased skeletal muscle fatty acid oxidation (Wang *et al.*, 2003). In diabetic db/db mice, a long-term PPARβ activation improves insulin sensitivity and islet function along with an improved lipid profile, suggesting that PPARβ activation might be a target for the treatment of type 2 diabetes (Winzell *et al.*, 2010).

Several lines of evidence indicate that activation of PPARβ enhances insulin sensitivity in adipocytes and skeletal muscle cells improving the glucose metabolism and the lipid profile (Leibowitz *et al.*, 2000; Oliver Jr *et al.*, 2001; Tanaka *et al.*, 2003; Wang *et al.*, 2003; Krämer *et al.*, 2005; Fritz *et al.*, 2006; Coll *et al.*, 2010; Serrano-Marco *et al.*, 2011). There are also studies reporting the opposite or no effects of PPARβ stimulation in different *in vitro* models (Brunmair *et al.*, 2006; Terada *et al.*, 2006; Dimopoulos *et al.*, 2007; Cresser *et al.*, 2010). However, whether PPARβ activation affects insulin signalling in endothelial cells is not known. Therefore, we examined the possible protective effects of PPARβ agonists on impaired insulin signalling induced *in vitro* by high glucose in cultured primary HUVECs, and *in vivo* in arterial vessels from diabetic rats.

Methods

Cell cultures

Endothelial cells were isolated from human umbilical cord veins using a previously reported method with several modifications (Jiménez *et al.*, 2010). The cells were cultured (Medium 199 + 20% FBS + penicillin/streptomycin 2 mmol L^{-1} + amphotericin B 2 mmol L^{-1} + glutamine 2 mmol L^{-1} + HEPES 10 mmol L^{-1} + endothelial cell growth supplement 30 μg·mL^{-1} + heparin 100 mg·mL^{-1}) under 5% CO_2 at 37°C. HUVECs were incubated with the PPARβ agonists, GW0742 and L165041 (1 or 10 μmol·L^{-1}), or the PPARα agonist, clofibrate (1 μmol·L^{-1}), the PPARγ agonist, ciglitazone (1 μmol·L^{-1}), the ERK)/2 inhibitor, PD98059 (10 μmol·L^{-1}), or the c-Jun N-JNK inhibitor, SP600125 (25 μmol·L^{-1}), for 24 h in low (5 mmol L^{-1})- or high (30 mmol L^{-1})-glucose medium. In some experiments, cells were co-incubated with the PPARβ antagonist, GSK0660 (1 μmol·L^{-1}), for 1 h before the addition of each PPARβ agonist. Cells were then used to measure NO production by diaminofluorescein-2 (DAF-2) fluorescence or to analyse protein expression or phosphorylation by Western blot under basal conditions or after the exposure to insulin (500 nmol·L^{-1}).

Transfection of PPARβ and PDK4 siRNAs

Confluent HUVECs were transfected with control, PPARβ- or PDK4-specific siRNA (pooled, validated siRNA from Dharmacon, Lafayette, CO, USA) using Lipofectamine RNAiMAX (Invitrogen Life Technologies, Carlsbad, CA, USA) for 48 h, essentially as described previously (Piqueras *et al.*, 2009).

Quantification of NO released by DAF-2

Quantification of NO released by HUVECs was performed using the NO-sensitive fluorescent probe DAF-2 as described previously (Jiménez *et al.*, 2010). Briefly, cells were incubated

as mentioned above for 24 h. After this period, cells were washed with PBS and then were pre-incubated with L-arginine (100 μmol·L^{-1} in PBS, 5 min, 37°C). Subsequently, the samples were incubated with DAF-2 (0.1 μmol·L^{-1}) for 2 min and then either insulin (500 nmol·L^{-1}) or the calcium ionophore calimycin (A23187, 1 μmol·L^{-1}) was added and cells were incubated in the dark at 37°C for 30 min. Then the fluorescence was measured using a spectrofluorimeter (Fluorostart, BMG Labtechnologies, Offenburg, Germany). The auto-fluorescence was subtracted from each value.

Protein expression and phosphorylation

Cells were incubated as mentioned above for 12 h for ERK1/2 analysis or 24 h for the rest of proteins or submitted to the siRNA procedure for 48 h. Then Western blotting was performed as described previously (Jiménez *et al.*, 2010).

Reverse transcriptase-PCR (RT-PCR) analysis

For RT-PCR analysis, total RNA was extracted from HUVECs by homogenization and converted to cDNA by standard methods. PCR was performed with a Techne Techgene thermocycler (Techne, Cambridge, UK). A quantitative real-time RT-PCR technique was used to analyse mRNA expression (Zarzuelo *et al.*, 2011). The sequences of the primers used for amplification of HUVECs samples are: PPARβ, sense CAT TGAGCCCAAGTTCGAGT, and antisense GGTTGACCTG CAGATGGAAT; PDK4, sense AGGTCGAGCTGTTCTCCC GCT and antisense GCGGTCAGGCAGGATGTCAAT, Mn-superoxide dismutase (MnSOD) sense GCCGTAGCTTCTC CTTAAA and antisense GCTACGTGAACAACCTGAA and for rat aorta samples, sense CCTAAGGGTGGTGGAGAACC and antisense CTGTGGTTCCTTGCAGTGG. Relative quantification of these different transcripts was determined with the ΔΔCt method using GAPDH and β-actin as endogenous control, respectively, and normalized to control group.

Measurement of intracellular reactive oxygen species (ROS) concentrations

The fluorescent probe 5-(and-6-)chloromethyl-2′-7′-dichlorodihydrofluorescein diacetate (CM-H2DCFDA) was used to determine the intracellular generation of ROS in endothelial cells. Confluent HUVEC in 96-well plates were grown in 5 or 30 mmol L^{-1} glucose in the presence or absence of either L165041 (1 μmol·L^{-1}), the inhibitor of complex I rotenone (5 μmol·L^{-1}), the inhibitor of complex II, thenoyltrifluoroacetone (TTFA 10 μmol·L^{-1}), or the uncoupler of oxidative phosphorylation, carbonyl cyanide m-chlorophenylhydrazone (CCCP, 0.5 μmol·L^{-1}) for 24 h. Inhibitors (GSK0660 1 μmol·L^{-1}), dichloroacetate (DCA) 10 μmol·L^{-1} or the mitochondrial antioxidant mitoquinone (mitoQ, generously given by Dr. MP Murphy, Medical Research Council Mitochondrial Biology Unit, Cambridge, UK, 0.1 μmol·L^{-1}) were added and pre-incubated for 30 min for GSK0660 and DCA, and 60 min for mitoQ before the incubation with L165041. Thereafter, the cells were incubated with 5 μmol·L^{-1} CM-H2DCFDA for 30 min at 37°C. The fluorescent intensity was measured using a spectrofluorimeter (Fluorostart, BMG Labtechnologies, Offenburg, Germany).

Animals and experimental groups

The experimental protocol followed the European Union guidelines for animal care and protection and our Institutional Guidelines for the ethical care of animals (University of Granada, ref. 2066/10). Male Wistar rats, 280–320 g in weight, were maintained at a constant temperature (24±1 °C), with a 12-h dark/light cycle and on standard rat chow. The total number of animals used: 30.The rats were randomized to three experimental groups: untreated control group (vehicle, 1 mL of 1% methylcellulose), untreated diabetic (vehicle) and GW0742-treated diabetic group (5 mg·kg^{-1}day^{-1}, mixed in 1 mL of 1% methylcellulose, by oral gavage). Diabetic rats received a single injection via the tail vein of streptozotocin (STZ, 50 mg·kg^{-1} dissolved in a citrate buffer at pH, 4.5). Rats with blood glucose levels of 2 mg·mL^{-1} or above and polyuria were considered to be diabetic. GW0742 treatment was started 4 days after STZ injection, and the treatment continued for 3 days. All studies involving animals are reported in accordance with the ARRIVE guidelines for reporting experiments involving animals (Kilkenny *et al.*, 2010; McGrath *et al.*, 2010).

Vascular reactivity studies

Descending thoracic aortic rings (3 mm) and the third branch of the mesenteric artery (1.7–2 mm) were dissected from animals and were mounted in organ chambers and in a wire myograph respectively. After equilibration, vessels were contracted by phenylephrine (Phe, 1 μmol·L^{-1}) and concentration-relaxation response curves were performed by cumulative addition of insulin in the absence or presence (added 1 h before Phe) of the PDK4 inhibitor (DCA, 10 μmol·L^{-1}), or the mitochondrial antioxidant mitoQ (0.1 μmol·L^{-1}), or the endothelial NO synthase (eNOS) inhibitor N$^{\omega}$-nitro-L-arginine methyl ester (L-NAME, 100 μmol·L^{-1}, 15 min before Phe). The concentration-relaxation response curves to sodium nitroprusside were performed in the dark in aortic rings without endothelium, precontracted by the addition of 1 μmol·L^{-1} Phe.

In order to analyse eNOS and Akt phosphorylation, some aortic rings were incubated for 15 min with insulin (100 nmol·L^{-1}) in Krebs solution. Other rings were used to measure ERK1/2, AMPK and insulin receptor substrate (IRS)-1 phosphorylation, and PPARβ protein expression by Western blot (Jiménez *et al.*, 2010).

Statistical analyses

Values are expressed as mean ± SEM. Statistical comparisons were performed using Student's *t*-tests or one-way ANOVA with Bonferroni's procedure for *post hoc* analysis. Values of $P < 0.05$ were considered significant.

Results

High glucose inhibits insulin-stimulated NO production and Akt and eNOS phosphorylation

Exposure of HUVECs to insulin (0.1–500 nmol·L^{-1}) increased, in a concentration-dependent manner, the DAF-2

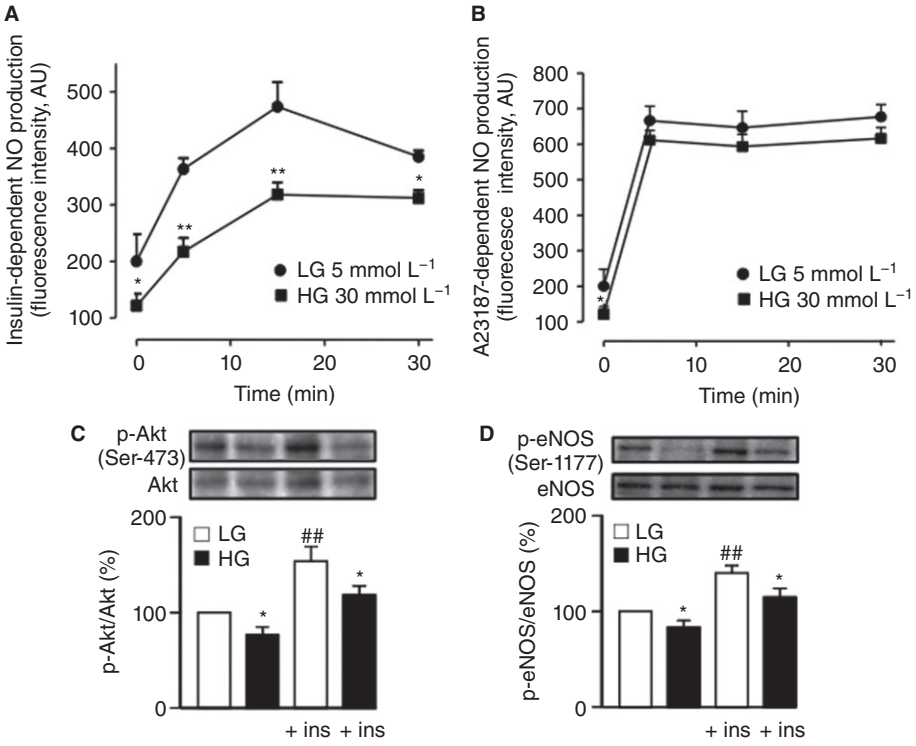

Figure 1

Impaired insulin signalling in HUVECs exposed to high glucose. NO released from HUVECs incubated for 24 h in low (LG, 5 mmol L^{-1})- or high (HG, 30 mmol L^{-1})-glucose medium was measured by DAF-2 fluorescence. Insulin (500 nmol·L^{-1}) (A) or the calcium ionophore calimycin (A23187, 1 μmol·L^{-1}) (B) were added at time 0. Results are mean ± SEM (n = 8) and *P < 0.05, **P < 0.01 versus cells exposed to LG. Expression of phospho-Akt (C) and phospho-eNOS (D) by Western blot in HUVECs in 5 or 30 mmol L^{-1} glucose, under basal- and insulin-stimulated (500 nmol·L^{-1} for 10 min) conditions. Results are means ± SEM (n = 4–6) of densitometric values normalized to the corresponding Akt or eNOS. *P < 0.05 versus low glucose and $^{\#\#}P$ < 0.01 insulin versus basal.

fluorescence intensity compared with non-stimulated cells (Supporting Information Figure S1A, Figure 1A). The fluorescent signal was abolished by the eNOS inhibitor L-NAME (100 μmol·L^{-1}, Supporting Information Figure S2A). Moreover, the PI3K inhibitor LY-294002 (10 μmol·L^{-1}) suppressed the insulin-increased DAF-2 fluorescence (Supporting Information Figure S2A). Incubation in high-glucose medium (10, 15 or 30 mmol L^{-1} for 24 h) reduced significantly both basal and insulin (500 nmol·L^{-1})-dependent NO production as compared with cells exposed to low glucose (Supporting Information Figure S1B, Figure 1A). In order to determine whether PPARβ activation was able to prevent the impairment of insulin signalling in extremely high-glucose levels, we performed the rest of experiments using 30 mmol L^{-1}. To investigate whether this inhibitory effect of high glucose was restricted to insulin-stimulated NO synthesis, we next examined the effect of high glucose on NO production stimulated by the calcium ionophore A23187 (Figure 1B). A23187 rapidly stimulated NO synthesis in HUVECs and there was no significant difference in the response of cells incubated at low- or high-glucose concentration. A23187-dependent NO production was abolished by eNOS inhibitor L-NAME or the intracellular Ca^{2+} quelator BAPTA-AM (10 μmol·L^{-1}) (Supporting Information Figure S2B). Insulin induced an increase in Akt (Figure 1C) and eNOS (Figure 1D) phosphorylation. Moreover, exposure of HUVECs to high glucose caused a reduction in the phosphorylation of both basal and insulin-stimulated Akt (Figure 1C) and eNOS (Figure 1D) phosphorylation.

PPARβ activation restores the high glucose-induced impairment of the insulin-Akt-eNOS pathway

When HUVECs were incubated in low-glucose medium for 24 h, co-incubation with PPARβ agonists, GW0742 or L165041 (1 or 10 μmol·L^{-1}), did not change NO production (Figure 2A,B) stimulated by insulin. However, both PPARβ agonists increased insulin-mediated NO production in HUVECs exposed to high-glucose medium (Figure 2C,D). These effects were suppressed when HUVEC were co-incubated with the PPARβ antagonist GSK0660 (1 μmol·L^{-1}). Both PPARβ agonists also increased insulin-stimulated Akt (Figure 2E) and eNOS (Figure 2F) phosphorylation and again these effects were prevented by GSK0660 (1 μmol·L^{-1}).

To confirm these observations further, in another set of experiments, HUVECs were treated with control or pooled, validated PPARβ siRNA. Forty-eight hours post-transfection with PPARβ-specific siRNA, HUVECs showed a >80% decrease in mRNA PPARβ (Figure 3A) and >85% protein (Figure 3B) relative to control siRNA-treated cells. PPARβ-specific, but not control, siRNA abolished the increase in insulin-stimulated

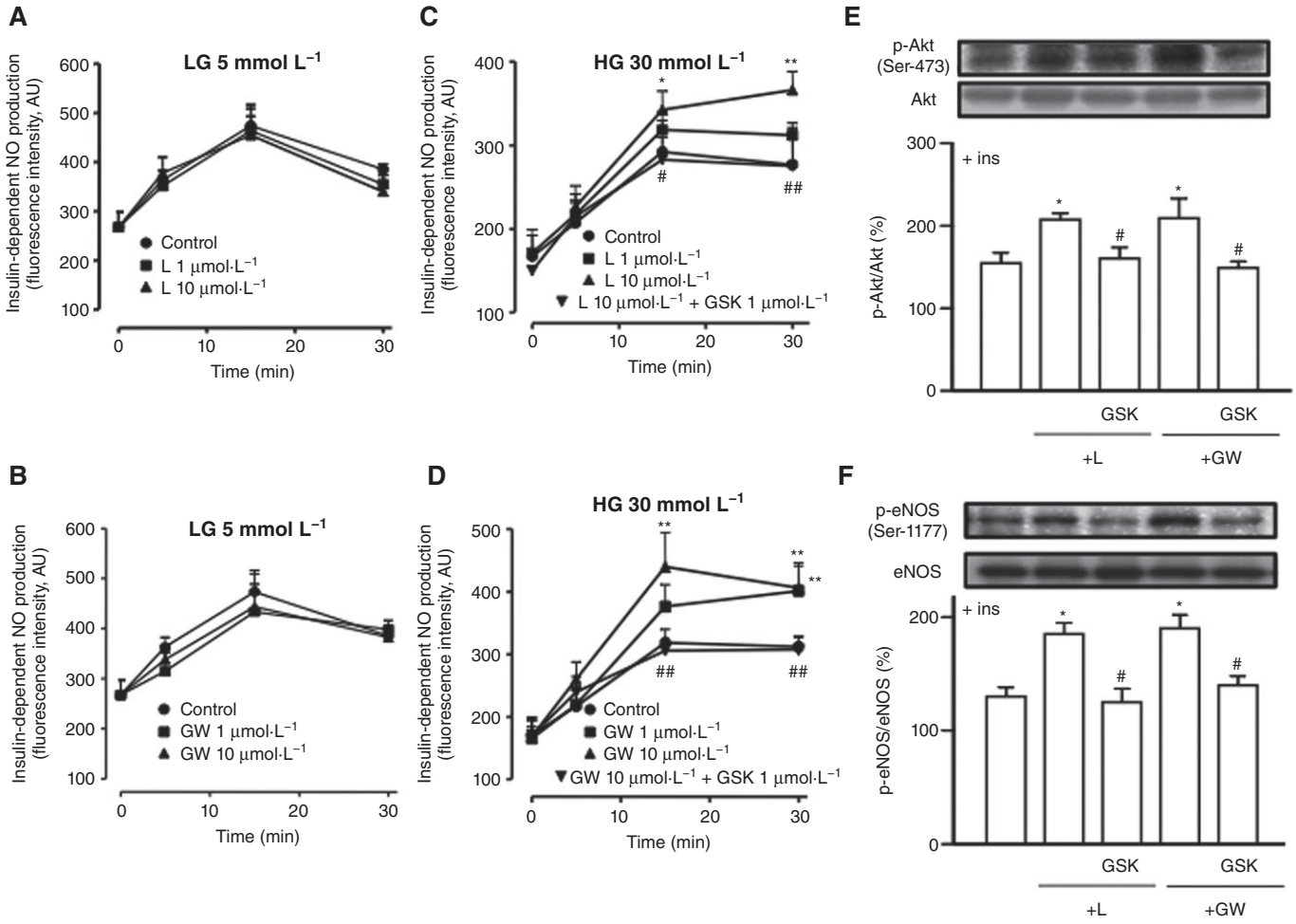

Figure 2

Effects of PPARβ agonists on impaired insulin signalling in high-glucose (HG) medium. Insulin-mediated NO production in HUVECs exposed to low-glucose (LG; 5 mmol L^{-1}, A and B) or high-glucose (30 mmol L^{-1}, C and D) medium for 24 h co-incubated with or without the PPARβ agonists, L165041 (L, 1 and 10 μmol·L^{-1}) (A and C) or GW0742 (GW, 1 and 10 μmol·L^{-1}) (B and D). Experiments were also performed in HUVECs co-incubated with the PPARβ antagonist GSK0660 (GSK, 1 μmol·L^{-1}). Akt (E) and eNOS (F) phosphorylation was measured in HUVECs exposed to HG medium for 24 h co-incubated with or without the PPARβ agonists (10 μmol·L^{-1}) and then with insulin for 10 min. All data are mean ± SEM (n = 8). Data presented as densitometric values protein band normalized to the corresponding Akt or to the corresponding eNOS. The protein bands are representative of n = 4–6.*P < 0.05 and **P < 0.01 versus control condition. $^{\#}P$ < 0.05 and $^{\#\#}P$ < 0.01 versus without GSK conditions.

NO production induced by both PPARβ ligands in cells incubated in high-glucose medium (Figure 3C).

To determine whether this protective effect on insulin-stimulated NO production is selective for PPARβ activation or it is shared by other PPARs, we next examined the effects of a selective PPARα, clofibrate, or a PPARγ ligand, ciglitazone. The incubation with either agent also prevented the decrease in insulin-stimulated NO synthesis induced by high glucose (Supporting Information Figure S3).

Role of 5′-AMP-activated protein kinase (AMPK) and MAPKs

To determine whether AMPK is involved in the protective effects of PPARβ agonists, we examined the effect of AMPK inhibitor, compound C, on insulin-stimulated NO production (Supporting Information Figure S4A) and the effects of PPARβ agonists on Thr-172 AMPK phosphorylation (Supporting Information Figure S4B). AMPK inhibition with previous incubation (1 h before NO determination) with compound C did not modify the increased insulin-stimulated NO production induced by both GW0742 and L165041 (10 μmol·L^{-1}) in HUVECs exposed to high glucose (Supporting Information Figure S4A). Moreover, AMPK phosphorylation was not altered by high-glucose medium and neither GW0742 nor L165041 induced any change in AMPK phosphorylation (Supporting Information Figure S4B).

To explore the role of MAPKs, we analysed the effects of the ERK1/2 inhibitor, PD98059 (10 μmol·L^{-1}), or the JNK inhibitor, SP600125 (25 μmol·L^{-1}) in insulin-stimulated NO production in HUVECs incubated in high-glucose medium (Supporting Information Figure S4C). ERK1/2 inhibition restored the insulin-stimulated NO synthesis while the JNK

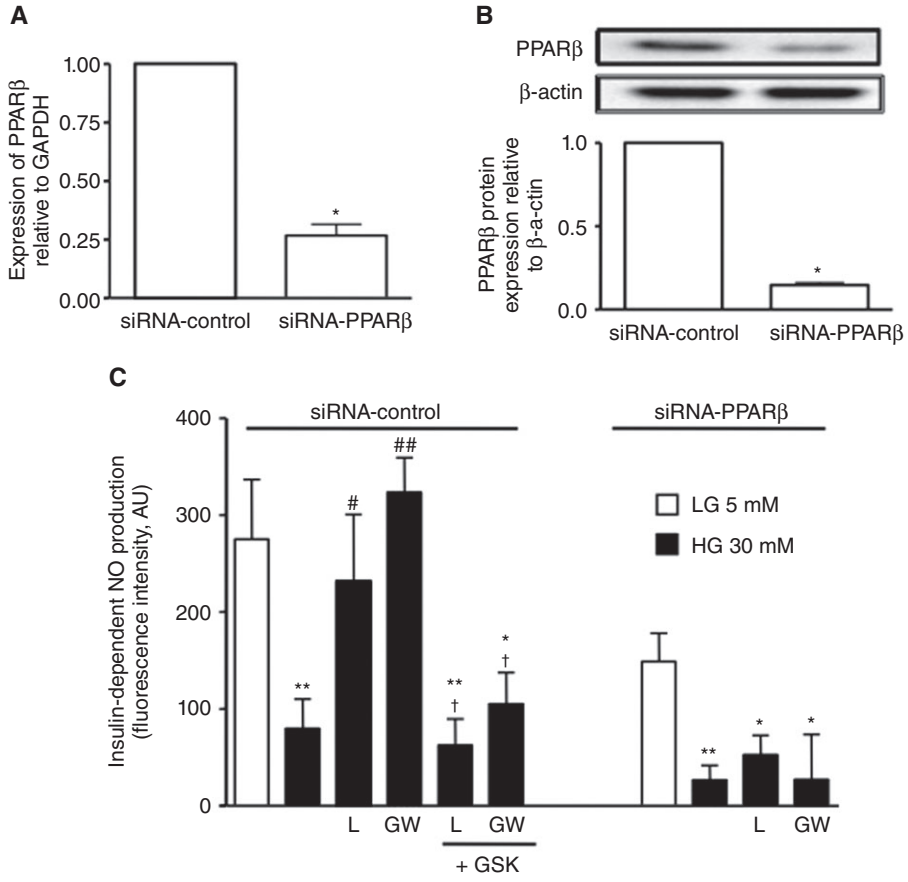

Figure 3

siRNA knockdown of PPARβ abolishes the effects of the PPARβ agonists. Expression of PPARβ at the level of mRNA determined by real-time RT-PCR (A) and protein by Western blot (B) in HUVECs transfected with either PPARβ-specific siRNA (siRNA-PPARβ) or empty vector (siRNA-control). Data are presented as gene expression normalized to GAPDH levels or densitometric protein band and normalized to the corresponding β-actin. Results are representative of $n = 4$ independent experiments. $^{*}P < 0.05$ versus siRNA-control. Insulin-mediated NO production (C) in control siRNA and siRNA-PPARβ cells incubated in low-glucose (LG) or high-glucose (HG) medium for 24 h, in the presence or absence of GW0742 or L165041 (10 μmol·L^{-1}) alone or pre-incubated with GSK0660 (1 μmol·L^{-1}). All data are mean ± SEM ($n = 8$). $^{**}P < 0.01$ versus LG medium. $^{\#}P < 0.05$ and $^{\#\#}P < 0.01$ versus without PPARβ agonist in HG medium. $^{\dagger}P < 0.05$, versus L or GW column.

inhibitor was without effect. Moreover, high glucose-induced ERK1/2 phosphorylation at 12 h was suppressed by co-incubation with either 10 μmol·L^{-1} GW0742 or 10 μmol·L^{-1} L165041 (Supporting Information Figure S4D).

Role of PPARβ target genes, carnitine palmitoiltransferase (CPT)-1 and PDK-4

We analysed the role of the PPARβ target genes CPT-1 and PDK4 in the effects of the PPARβ agonists by measuring insulin-stimulated NO production in high-glucose medium in the presence of etomoxir, an irreversible inhibitor of CPT-1, or DCA, an inhibitor of PDK4. In these experimental conditions, DCA abolished the increased NO production induced by both GW0742 and L165041 while etomoxir was without effect (Figure 4A). PDK4 mRNA levels were also increased in a concentration-dependent manner by either GW0742 (Figure 4B) or L165041 (Figure 4C), in HUVECs incubated in low- and high-glucose conditions. This effect was abolished by co-incubation with the PPARβ antagonist GSK0660. To confirm these observations further, in another set of experiments, HUVECs were treated with control or pooled, validated PDK4 siRNA. Forty-eight hours post-transfection with PDK4-specific siRNA, HUVECs showed a > 70 % decrease in PDK4 protein (Figure 4D) relative to control siRNA-treated cells. PDK4-specific, but not control, siRNA abolished the increase in insulin-stimulated NO production induced by both PPARβ ligands in cells incubated in high-glucose medium (Figure 4D).

Effects of PPARβ agonists on intracellular ROS production

To test whether the protective effects of PPARβ agonist L165041 might be related to inhibition of ROS, we measured intracellular ROS in HUVECs incubated in low- and high-glucose medium. Compared with baseline conditions (5 mmol L^{-1} glucose), incubation with 30 mmol L^{-1} glucose increased ROS production (Figure 5A). Rotenone did not reduce this increased ROS production, whereas TTFA, CCCP

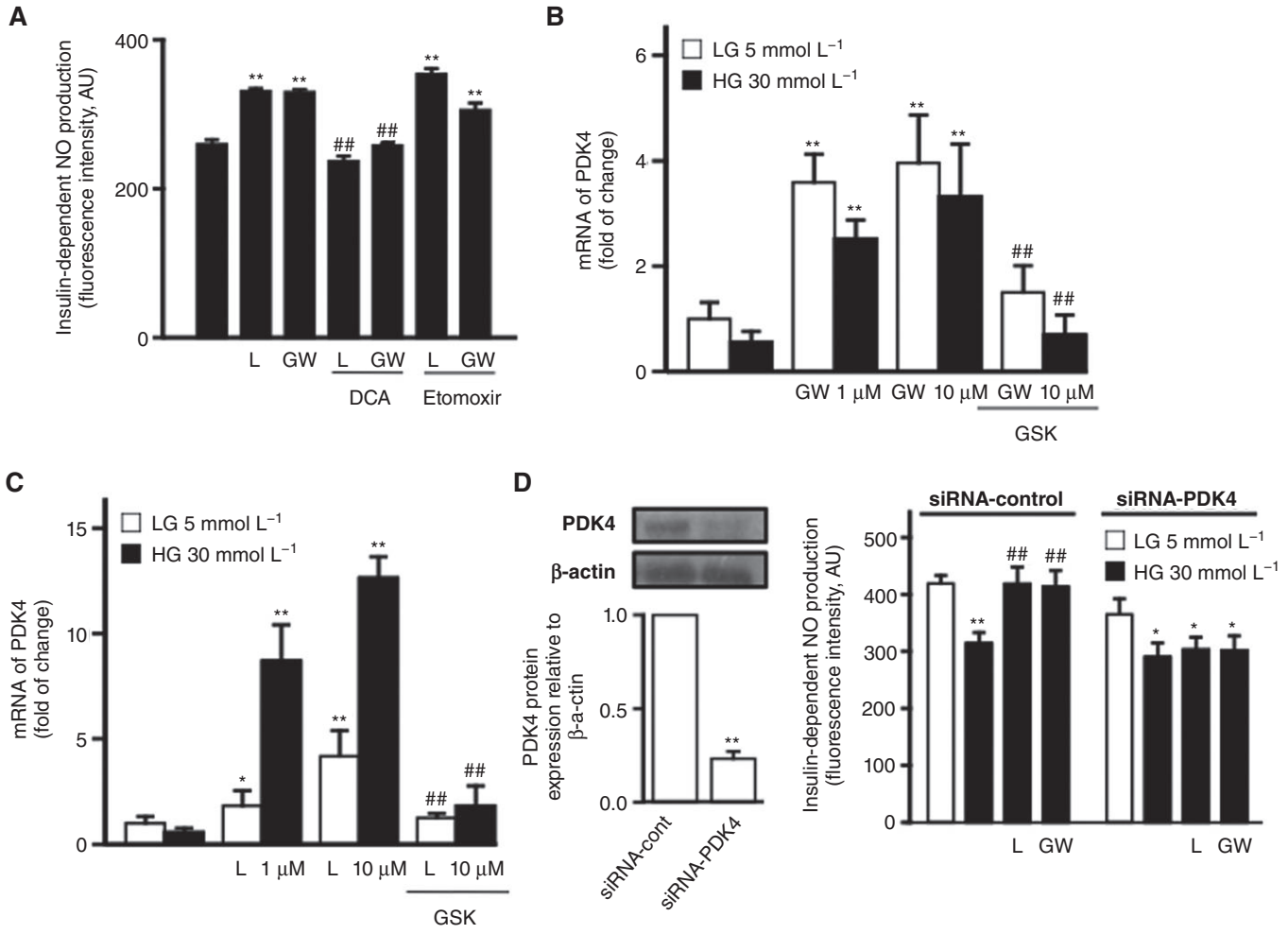

Figure 4

Role of the PPARβ target genes, CPT-1 and PDK4 in the protective effects of PPARβ agonists. Insulin-mediated NO production (A) and mRNA expression of PDK4 by real-time RT-PCR (B, C) in HUVECs exposed to low (5 mmol L^{-1}, LG) or high-glucose (30 mmol L^{-1}, HG) medium for 24 h with or without the PPARβ agonists, L165041 or GW0742 (10 μmol·L^{-1}), alone or pre-incubated with an irreversible inhibitor of CPT-1, etomoxir (40 μmol·L^{-1}) or an inhibitor of PDK4, DCA (10 μmol·L^{-1}) 30 min before measuring the insulin-mediated NO production at 15 min. (D) Left, expression of PDK4 protein by Western blot in HUVECs transfected with either PDK4-specific siRNA (siRNA-PDK4) or empty vector (siRNA-control). Data are presented as densitometric protein band and normalized to the corresponding β-actin. Results are representative of $n = 4$ independent experiments. $^{**}P < 0.01$ versus siRNA-control. Right, insulin-mediated NO production in control siRNA and siRNA-PDK4 cells incubated in LG or HG medium for 24 h, in the presence or absence of GW0742 or L165041 (10 μmol·L^{-1}). All data are mean ± SEM ($n = 8$). mRNA data presented as a ratio of arbitrary units of mRNA ($2^{-\Delta\Delta Ct}$). $^{*}P < 0.05$ and $^{**}P < 0.01$ versus control condition, $^{\#\#}P < 0.01$ versus L and GW column respectively.

and mitoQ completely prevented the effect of high glucose. Incubation with L165041 (1 μmol·L^{-1}) also abolished high glucose-induced intracellular ROS production. Co-incubation of this PPARβ agonist with either GSK0660 or DCA suppressed the inhibition of ROS production induced by L165041 in high-glucose medium. Moreover, both PPARβ- (Figure 5B) and PDK4-specific, (Figure 5C) but not control, siRNA abolished the inhibitory effect of L165041 in high glucose-induced mitochondrial ROS overproduction. In addition, MnSOD mRNA levels were increased in HUVECs incubated with L165041 and GW0742 in both low- and high-glucose conditions (Figure 5D).

To test if mitochondrial ROS are involved in ERK1/2 activation, we analysed ERK1/2 phosphorylation in HUVECs incubated in the presence of TTFA or catalase. Both agents suppressed the increased ERK1/2 phosphorylation induced by high glucose (Figure 5E).

Effects of PPARβ agonists on IRS phosphorylation

High glucose increased both Ser^{636}-IRS-1 (Figure 6A) and Ser^{270}-IRS1/2 (Figure 6B) phosphorylation in HUVEC. This effect was abolished by the presence of PPARβ agonists GW0742 or L165041 (Figure 6). Co-incubation with the PPARβ antagonist, GSK0660, restored the level of phosphorylation induced by high glucose. Interestingly, the presence of the ERK1/2 inhibitor, PD98059, also suppressed the increase in IRS-1/2 phosphorylation induced by high glucose.

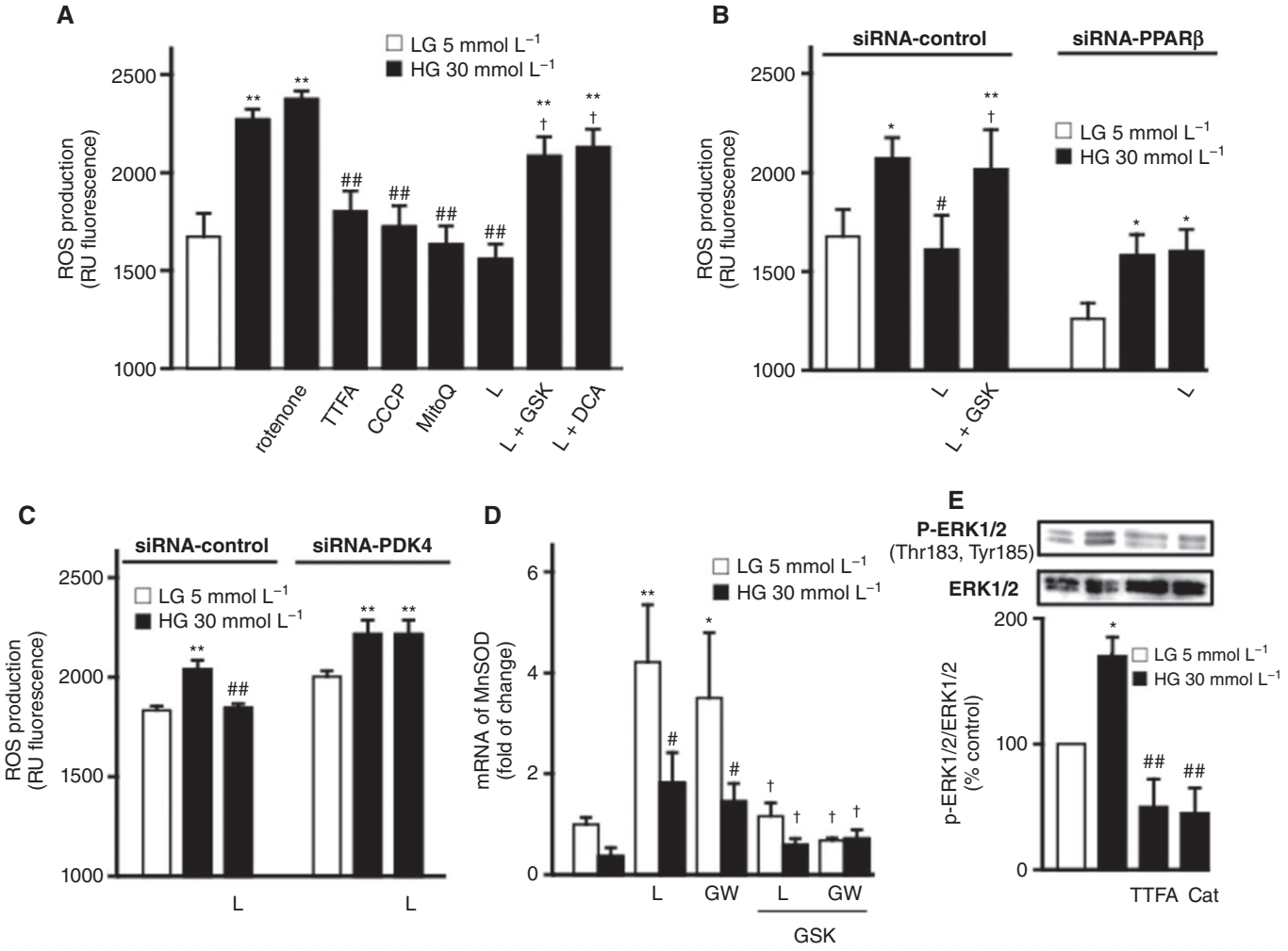

Figure 5

Effects of the PPARβ agonists in intracellular ROS production. CM-H2DCFDA-detected intracellular ROS in HUVECs (A) and HUVEC transfected with PPARβ-specific siRNA (siRNA-PPARβ) (B), or with PDK4-specific siRNA (siRNA-PDK4) (C) incubated in low (5 mmol L^{-1}, LG) or high-glucose (30 mmol L^{-1}, HG) medium for 24 h in the presence or absence of either L165041 (1 μmol·L^{-1}), the inhibitor of complex I rotenone (5 μmol·L^{-1}), the inhibitor of complex II, thenoyltrifluoroacetone (TTFA 10 μmol·L^{-1}), or the uncoupler of oxidative phosphorylation, carbonyl cyanide m-chlorophenylhydrazone (CCCP, 0.5 μmol·L^{-1}). Inhibitors (GSK0660 1 μmol·L^{-1}, DCA 10 μmol·L^{-1}, or mitoQ 0.1 μmol·L^{-1}) were added 30 (GSK0660 and DCA) or 60 min (mitoQ) before the incubation with L165041. (D) mRNA expression of MnSOD by real-time RT-PCR in HUVECs exposed to LG (5 mmol L^{-1}) or HG (30 mmol L^{-1}) medium for 24 h with or without the PPARβ agonists, L165041 or GW0742 (10 μmol·L^{-1}) alone or co-incubated with the PPARβ antagonist GSK0660 (GSK, 1 μmol·L^{-1}). (E) ERK1/2 phosphorylation in HUVECs incubated in the presence of TTFA and catalase. Data represent the mean ± SEM ($n = 8$), and the experiments were repeated independently at least three times. Data presented as densitometric values protein band normalized to the corresponding ERK 1/2; the bands are representative of $n = 3$–5. $^{*}P < 0.05$ and $^{**}P < 0.01$ versus LG medium respectively. $^{\#}P < 0.05$ and $^{\#\#}P < 0.01$ versus HG medium. $^{\dagger}P < 0.05$ versus L or GW column without inhibitor.

GW0742 treatment in vivo *improves insulin-induced vasodilatation in STZ-induced diabetic rats in a PDK4-dependent manner*

GW0742 treatment did not modify the increase in plasma glucose (Figure 7A) induced by STZ injection but increased the expression of aortic PDK4 and MnSOD (Figure 7B). ERK1/2 and Ser^{636}-IRS-1 phosphorylation was increased in diabetic rats, and restored at control values after GW0742 treatment (Supporting Information Figure S5). No significant changes were observed among groups in AMPK phosphorylation. However, aortic PPARβ protein expression was increased in STZ group and significantly increased by GW0742 treatment (Supporting Information Figure S5). Akt and eNOS phosphorylation induced by insulin were decreased in aorta from STZ rats compared with controls and these changes were prevented by GW0742 (Figure 7C). In the aorta (Figure 7D) and the mesenteric resistance arteries (Figure 7E) isolated from diabetic rats, the relaxations induced by insulin were reduced. In vessels from diabetic rats treated with GW0742, the relaxations induced by insulin were preserved. Treatment of the arteries *in vitro* with mitoQ also restored the relaxation. The improvement of insulin relaxation induced by GW0742

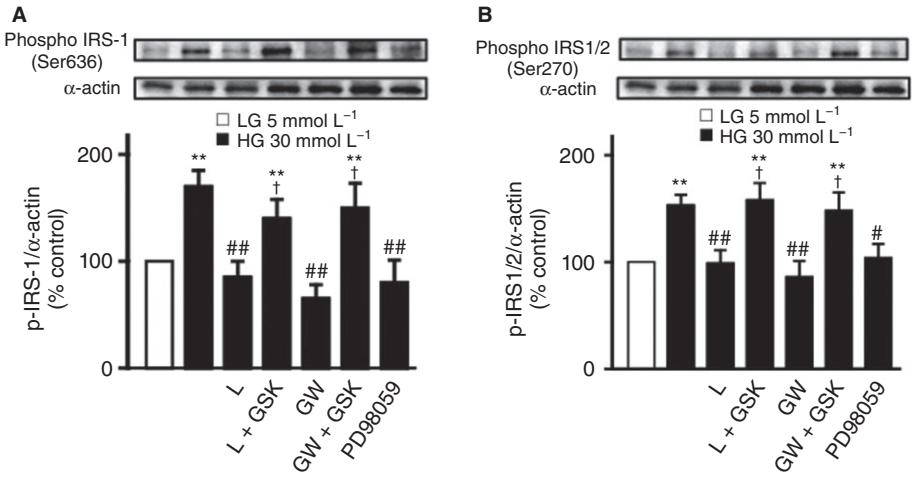

Figure 6

Effects of PPARβ agonists on IRS phosphorylation. Ser^{636}-IRS-1 (A) or Ser^{270}-IRS-1/2 (B) phosphorylation by Western blot in HUVECs incubated in low (5 mmol L^{-1}, LG) or high-glucose (30 mmol L^{-1}, HG) medium for 24 h with or without the PPARβ agonists, L165041 (L, 10 μmol·L^{-1}) or GW0742 (GW, 10 μmol·L^{-1}), alone or pre-incubated with the PPARβ antagonist GSK0660 (1 μmol·L^{-1}) or the ERK1/2 inhibitor, PD98059 (10 μmol·L^{-1}). Data presented as densitometric values, protein band normalized to the corresponding α-actin; the bands are representative of $n = 3–5$. $^{\#}P < 0.05$ and $^{**}P < 0.01$ versus LG medium. $^{\#\#}P < 0.01$ versus drug free in HG medium. $^{\dagger}P < 0.05$ versus L and GW column respectively.

was suppressed when the vessels were incubated with the PDK4 inhibitor DCA. These relaxant responses to insulin in aortic rings were suppressed by the NOS inhibitor L-NAME (100 μmol·L^{-1}) (Supporting Information Figure S6A). Endothelium-independent relaxations to nitroprusside were similar among groups (Supporting Information Figure S6B).

Discussion and conclusions

Several lines of evidence indicate that activation of PPARβ enhances insulin sensitivity in adipocytes and skeletal muscle cells (Leibowitz *et al.*, 2000; Oliver Jr *et al.*, 2001; Tanaka *et al.*, 2003; Wang *et al.*, 2003; Krämer *et al.*, 2005; Fritz *et al.*, 2006; Coll *et al.*, 2010; Serrano-Marco *et al.*, 2011). Herein, we report that in human endothelial cells and rat arteries activation of PPARβ via PDK4 up-regulation prevented the high glucose-induced impairment of insulin-stimulated NO production and relaxation. This protective effect seems to be related to the inhibition of mitochondrial ROS production and ERK1/2 activation.

Insulin receptor activation (Figure 8) results in phosphorylation of multiple tyrosine residues of IRS-1, which then activates PI3K, leading to phosphorylation and activation of protein kinase (PDK1). PDK1, in turn, phosphorylates and activates Akt, which finally phosphorylates eNOS at the activator site Ser1177 increasing eNOS activity and NO production (Vincent *et al.*, 2003). In endothelial cells exposed to high glucose, the insulin-stimulated NO production is impaired (Schnyder *et al.*, 2002; Salt *et al.*, 2003; Kim *et al.*, 2005), but the mechanisms are not fully characterized. It has been reported that high glucose inhibits basal eNOS expression, activity and NO production in cultured endothelial cells (Ding *et al.*, 2000; Du *et al.*, 2001). This has been related to increased ROS production which may decrease NO via different mechanisms (Muniyappa and Quon, 2007): (i) direct decrease of NO bioavailability (e.g. the direct reaction of NO with superoxide), (ii) reduction of cellular tetrahydrobiopterin levels promoting eNOS uncoupling, (iii) formation of advanced glycation end-products, which inhibit the PI3K/Akt/eNOS pathway and accelerate eNOS mRNA degradation (Xu *et al.*, 2003; Wallis *et al.*, 2005; Goldin *et al.*, 2006), (iv) O-linked N-acetylglucosaminylation of eNOS at the Akt phosphorylation site at Ser^{1179} resulting in impaired eNOS activity (Du *et al.*, 2001), and (v) stimulation of Ser^{636} phosphorylation of IRS-1 which reduces the binding of p85 regulatory subunit of PI3K to IRS-1 and promoting insulin resistance (Esposito *et al.*, 2001). MAPKs, such as ERK1/2 and JNK, are stress-activated protein kinases, which may interfere with insulin signalling by phosphorylation of IRS-1 at Ser^{636} (Rains and Jain, 2011). In our experimental conditions, high glucose reduced both insulin-dependent NO production and (Ser^{473})-Akt and (Ser^{1177})-eNOS phosphorylation as compared with cells exposed to low glucose. This effect was restricted to insulin-stimulated eNOS activation because the A23187-induced NO production was unaffected by high glucose. Our results are in agreement with the hypothesis involving the increase in mitochondrial ROS production, the subsequent ERK1/2 phosphorylation and the IRS-1 (Ser^{636}) and IRS-1/2 (Ser^{270}) phosphorylation in the impairment of insulin-stimulated NO production. This is further supported by several findings. First, TTFA, an inhibitor of complex II of mitochondrial electron transport chain, and CCCP, an uncoupler of oxidative phosphorylation, and the mitochondrial antioxidant mitoQ inhibited high glucose-induced increase in ROS production (current results and Nishikawa *et al.*, 2000) and increased insulin-stimulated NO production. Second, in agreement with previous results (Chen *et al.*, 2007), high glucose increased ERK1/2 phosphorylation in HUVECs and in aorta from STZ group, which was inhibited

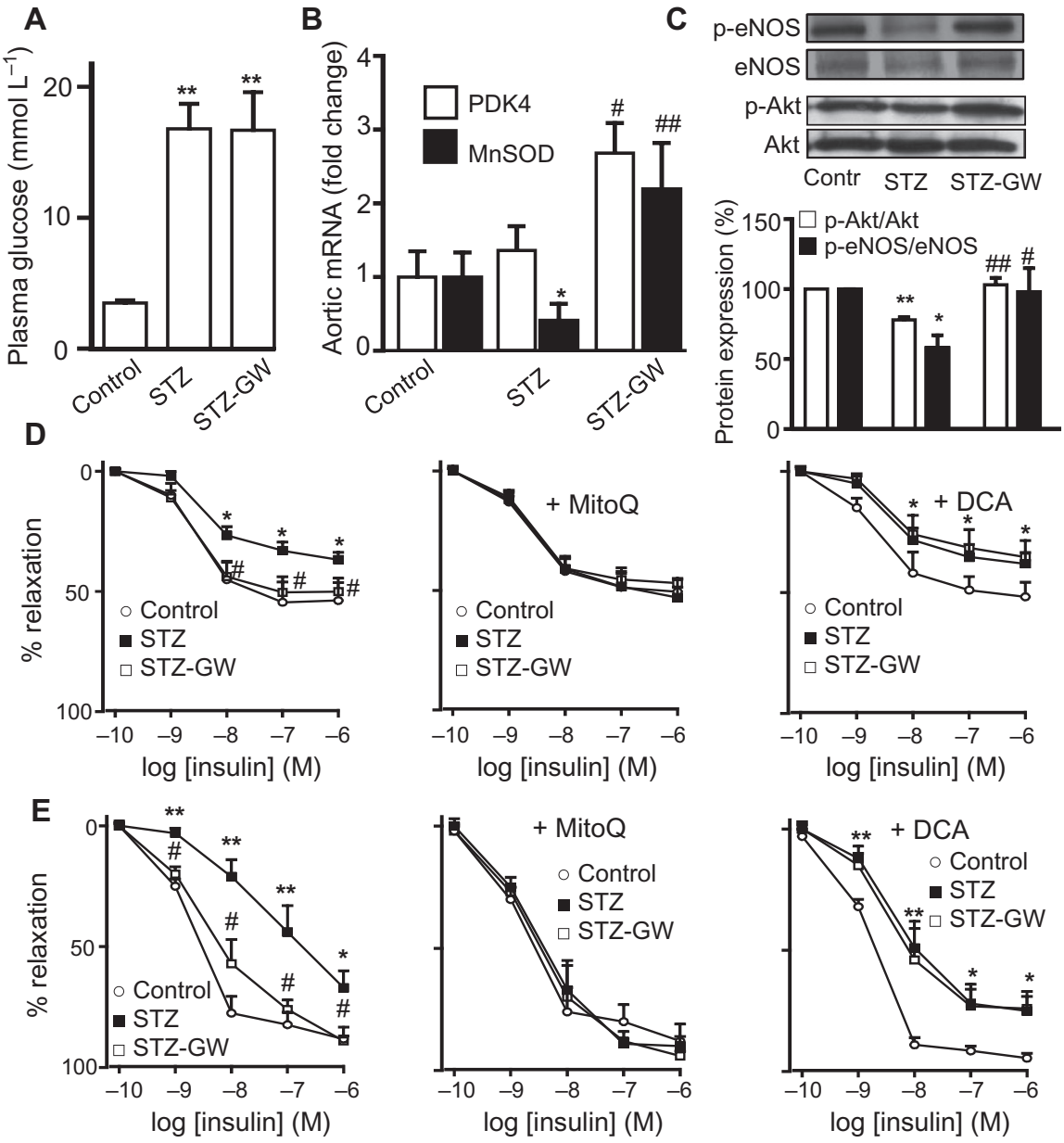

Figure 7

GW0742 treatment *in vivo* restored NO-mediated relaxation induced by insulin in vessels from streptozotocin (STZ)-induced diabetic rats. GW0742 (5 mg·kg^{-1}·day^{-1} for 3 days) treatment was started 4 days after STZ injection. Plasma glucose levels (A), and mRNA aortic expression of PDK4 and MnSOD by real-time RT-PCR (B). Phosphorylation of eNOS and Akt induced by insulin (100 nM) in aorta (C). Relaxation induced by insulin in aorta (D) and in mesenteric arteries (E) precontracted by phenylephrine (Phe, 1 μmol·L^{-1}), in the absence or presence of the PDK4 inhibitor (DCA, 10 μmol·L^{-1}), or the mitochondrial antioxidant mitoQ (0.1 μmol·L^{-1}) for 1 h before Phe. All data are mean ± SEM (n = 10). *P < 0.05 and **P < 0.01 versus control (non-diabetic rats treated with vehicle) group, $^{\#}P$ < 0.05 and $^{\#\#}P$ < 0.01 versus STZ respectively.

by TTFA and by the H_2O_2 scavenger catalase, suggesting that ERK1/2 is activated by ROS. ERK1/2 inhibition by PD98059 also increased insulin-stimulated NO production in HUVECs incubated in high-glucose medium, being without effect the JNK inhibitor, SP600125. Third, serine phosphorylation of IRS-1/2 was stimulated by high glucose in HUVECs and in aorta from diabetic rats, and inhibited by the ERK1/2 inhibitor PD98059.

In agreement with Quintela *et al*. (2012), the protein expression of PPARβ increased in the aorta from diabetic as compared with control rats, and was up-regulated by GW0742 treatment. Activation of PPARβ prevented the high glucose-induced impairment of the insulin signal to produce NO and arterial relaxation. This is supported by several data. First, PPARβ agonists, GW0742 and L165041, increased the NO production stimulated by insulin in high glucose cultured cells, being without effect in cells incubated in low glucose. This improvement in endothelial function was accompanied by increased Akt and eNOS phosphorylation. Second, *in vivo* GW0742 treatment also increased Akt and

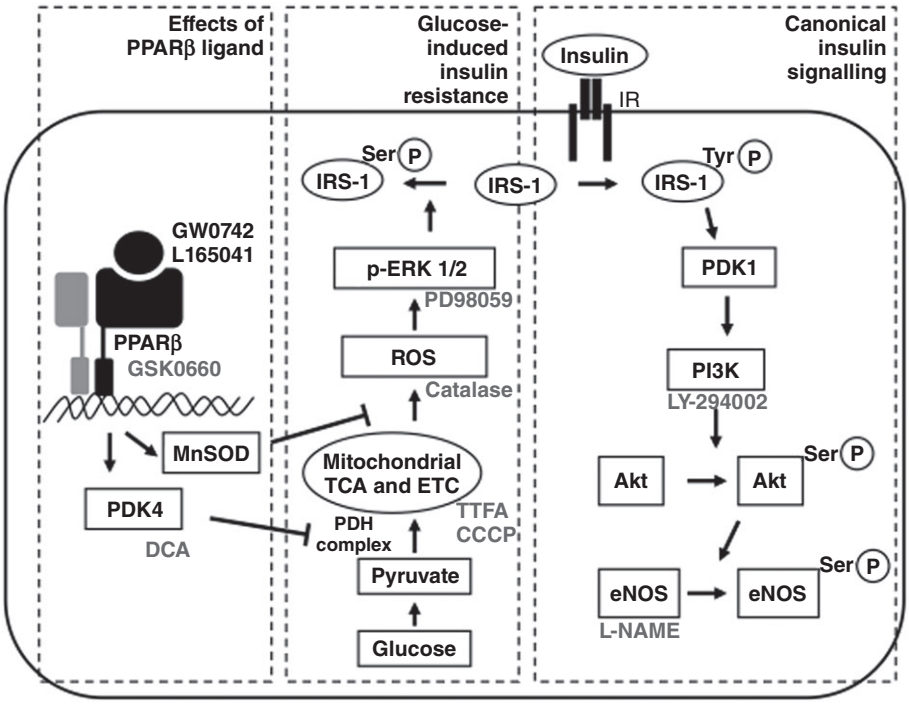

Figure 8

Scheme representing the insulin signalling pathway, the mechanisms involved in the high glucose-induced impairment of the insulin pathway and the proposed mechanism by which PPARβ agonists prevent high glucose-induced insulin resistance in HUVECs.

eNOS phosphorylation and improved NO-dependent insulin relaxation in aorta and mesenteric arteries from STZ rats. Similar results showing that PPARβ activation protects endothelial function and improves insulin-induced relaxation in diabetic and obese mice have been previously described (Tian *et al.*, 2012). However, these authors did not establish a clear link between the improvement of insulin relaxation and changes in insulin-stimulated PI3K/Akt/eNOS pathways. Our results are consistent with the mechanism of the physiological actions of insulin on the vascular endothelium, which is predominantly mediated via the IRS/PI3K/Akt pathway (as described above). Third, the activation of PPARβ by the agonists in these experiments is demonstrated by the up-regulation of PDK4, a canonical PPARβ target gene. Both functional and expressional effects induced by both agonists were suppressed when HUVEC were co-incubated with the PPARβ antagonist GSK0660. Moreover, PPARβ-specific siRNA also abolished the protective effects of PPARβ agonists in insulin-stimulated NO production. This protective effect on NO production was not restricted to PPARβ activation, as a similar effect was also evoked by either PPARα agonist clofibrate or PPARγ ciglitazone.

Several mechanisms have been involved on the protective effects of PPARβ agonists on insulin resistance, such as activation of AMPK (Barroso *et al.*, 2011), ERK1/2 inhibition (Rodríguez-Calvo *et al.*, 2008) and CPT-1 activation (Coll *et al.*, 2010). AMPK is a metabolic sensor that detects low ATP levels and in turn increasing oxidative metabolism (Reznick and Shulman, 2006) by reducing the levels of malonyl-CoA, which inhibits CPT-1 activity. High glucose increases ATP synthesis by the mitochondria, leading to AMPK inhibition, at least, in rat mesangial cells (Lv *et al.*, 2012), which might induce a reduction in eNOS Ser-1177 phosphorylation and bioactivity (Thors *et al.*, 2008). However, in our experimental conditions, no changes in AMPK phosphorylation/activation were found. The PPARβ ligand GW5015116 increased the AMPK to ATP ratio in liver (Barroso *et al.*, 2011) and skeletal muscle cells (Krämer *et al.*, 2007) increasing AMPK phosphorylation. Our present data in HUVECs, in hyperglycaemic conditions, are in disagreement with these previous evidences, as no significant increase in AMPK phosphorylation were found after either GW0742 or L165041 treatment, and also no change in the effects of both PPARβ agonists improving insulin-stimulated NO production was detected after AMPK inhibition by compound C. Moreover, AMPK phosphorylation was unchanged in aorta from STZ as compared with control rats.

As described above ERK1/2 activation seems to be involved in the impaired insulin signalling induced by high glucose. Protective effects of PPARβ agonists in lipopolysaccharide-induced cytokine production in adipocytes (Rodríguez-Calvo *et al.*, 2008) and PDGF-induced rat vascular smooth muscle proliferation (Lim *et al.*, 2009) seem to be related to prevention of ERK1/2 phosphorylation. In our experiments, both PPARβ agonists reduced ERK1/2 activation induced by high glucose in HUVECs, and also prevented the increased serine phosphorylation of IRS-1/2. This data in endothelial cells confirms that PPARβ regulates phospho-ERK1/2 levels in several tissues. In fact, similar results were found in aorta from diabetic rats after GW0742

treatment. However, the molecular mechanisms by which PPARβ controls ERK1/2 activation are unclear. Inhibitory cross-talk between ERK1/2 and AMPK has been reported (Du *et al.*, 2008), which can be ruled out in our experiments, as both PPARβ agonists did not increased AMPK activity. ERK1/2 is a stress-sensitive serine/threonine protein kinase. In our experiments, ERK1/2 activation was inhibited by TTFA and catalase, suggesting a role for mitochondrial ROS as cellular stimuli for ERK1/2 activation.

The glucose metabolism begins with glycolysis generating NADH and pyruvate. Pyruvate can be transported into the mitochondria, where it is oxidized by the pyruvate dehydrogenase complex yielding acetyl-CoA, which enters the tricarboxylic acid cycle to produce NADH and $FADH_2$. Mitochondrial NADH and $FADH_2$ lead to ATP production through oxidative phosphorylation by the electron transport chain. Inhibition of pyruvate transport into the mitochondria inhibited hyperglycaemia-induced ROS production, indicating that the mitochondrial tricarboxylic acid cycle- electron transport chain complex is the major source for ROS generation (Nishikawa *et al.*, 2000). PDK4 is a key enzyme that mediates the shift from glycolytic to fatty acid oxidative metabolism via pyruvate dehydrogenase phosphorylation and subsequent inactivation (Patel and Korotchkina, 2006). PPARβ is a key regulator of PDK genes, in particular the PDK4 gene (Degenhardt *et al.*, 2007). In fact, we found that both PPARβ agonists increased in a concentration-dependent manner the mRNA levels of PDK4 in HUVECs in either low- or high-glucose medium, and this effect was inhibited by blocking PPARβ with GSK0660. Furthermore, *in vivo* GW0742 treatment also increased PDK4 expression in aorta from STZ rats. Moreover, inhibition of PDK4 by both DCA or by PDK4-specific siRNA suppressed the inhibitory effects of L165041 in high glucose-induced mitochondrial ROS overproduction and also inhibited the increased insulin-mediated NO production induced by PPARβ activation in high-glucose medium. In addition, DCA also suppressed the improvement of insulin relaxation induced by GW0742 in aorta and small mesenteric arteries from diabetic rats.

Overexpression of MnSOD completely prevented the effect of hyperglycaemia (Du *et al.*, 2001). We found that mRNA levels of MnSOD in high-glucose conditions *in vitro* and *in vivo* were reduced as compared with low glucose. Interestingly, activation of PPARβ increased MnSOD expression in vascular cells, which would collaborate to reduce mitochondrial ROS production.

Taking into account that insulin signalling in endothelial cells seems to play a pivotal role in the regulation of glucose uptake by skeletal muscle (Kubota *et al.*, 2011), activation of PPARβ, which improves endothelial insulin signalling inducing NO-dependent relaxation, may serve as a therapeutic strategy for ameliorating skeletal muscle insulin resistance. However, this improvement in insulin signalling found in aorta from STZ rats treated with GW0742 was unable to lower blood glucose, possibly as a result of insufficient plasma insulin levels derived from beta-cells destruction.

In summary, we demonstrated that PPARβ ligands, both *in vitro* and *in vivo*, through up-regulation of PDK4, prevent the high glucose-induced impairment of the PI3K-Akt-eNOS pathway, leading to increased NO production stimulated by insulin in HUVECs and in rat aorta and mesenteric arteries (Figure 8). PDK4 and MnSOD overexpression normalizes mitochondrial ROS production and ERK1/2 activity thereby restoring insulin-stimulated IRS-Akt-eNOS signalling.

Acknowledgements

This work was supported by grants from Comisión Interministerial de Ciencia y Tecnología (SAF2011-28150, SAF2010-22066-C02-01 and -02) and by the Ministerio de Ciencia e Innovación, Instituto de Salud Carlos III (Red HERACLES RD06/0009), Spain. M. J. Z. and A. M. Q. are holders of studentships from Spanish Ministry of Science and Education.

Conflicts of interest

None.

References

Alexander SPH, Benson HE, Faccenda E, Pawson AJ, Sharman JL, Spedding M, Peters JA, Harmar AJ and CGTP Collaborators (2013). The Concise Guide to PHARMACOLOGY 2013/14: Nuclear hormone receptors. Br J Pharmacol 170: 1652–1675.

Barroso E, Rodríguez-Calvo R, Serrano-Marco L, Astudillo AM, Balsinde J, Palomer X *et al.* (2011). The PPARβ activator GW501516 prevents the down-regulation of AMPK caused by a high-fat diet in liver and amplifies the PGC-1α-Lipin 1-PPARα pathway leading to increased fatty acid oxidation. Endocrinology 152: 1848–1859.

Boden G (2011). Obesity, insulin resistance and free fatty acids. Curr Opin Endocrinol Diabetes Obes 18: 139–143.

Braissant O, Foufelle F, Scotto C, Dauça M, Wahli W (1996). Differential expression of peroxisome proliferator-activated receptors (PPARs): tissue distribution of PPAR-alpha, -beta, and -gamma in the adult rat. Endocrinology 137: 354–366.

Brunmair B, Staniek K, Dörig J, Szöcs Z, Stadlbauer K, Marian V *et al.* (2006). Activation of PPAR-delta in isolated rat skeletal muscle switches fuel preference from glucose to fatty acids. Diabetologia 49: 2713–2722.

Chen YH, Guh JY, Chuang TD, Chen HC, Chiou SJ, Huang JS *et al.* (2007). High glucose decreases endothelial cell proliferation via the extracellular signal regulated kinase/p15(INK4b) pathway. Arch Biochem Biophys 465: 164–171.

Coll T, Alvarez-Guardia D, Barroso E, Gómez-Foix AM, Palomer X, Laguna JC *et al.* (2010). Activation of peroxisome proliferator-activated receptor-{delta} by GW501516 prevents fatty acid-induced nuclear factor-{kappa}B activation and insulin resistance in skeletal muscle cells. Endocrinology 151: 1560–1569.

Cresser J, Bonen A, Chabowski A, Stefanyk LE, Gulli R, Ritchie I *et al.* (2010). Oral administration of a PPAR-delta agonist to rodents worsens, not improves, maximal insulin-stimulated glucose transport in skeletal muscle of different fibers. Am J Physiol Regul Integr Comp Physiol 299: R470–R479.

Degenhardt T, Saramäki A, Malinen M, Rieck M, Väisänen S, Huotari A *et al.* (2007). Three members of the human pyruvate

dehydrogenase kinase gene family are direct targets of the peroxisome proliferator-activated receptor beta/delta. J Mol Biol 372: 341–355.

Desvergne B, Wahli W (1999). Peroxisome proliferator-activated receptors: nuclear control of metabolism. Endocr Rev 20: 649–688.

Dimopoulos N, Watson M, Green C, Hundal HS (2007). The PPARdelta agonist, GW501516, promotes fatty acid oxidation but has no direct effect on glucose utilisation or insulin sensitivity in rat L6 skeletal muscle cells. FEBS Lett 581: 4743–4748.

Ding Y, Vaziri ND, Coulson R, Kamanna VS, Roh DD (2000). Effects of simulated hyperglycemia, insulin, and glucagon on endothelial nitric oxide synthase expression. Am J Physiol Endocrinol Metab 279: E11–E17.

Du J, Guan T, Zhang H, Xia Y, Liu F, Zhang Y (2008). Inhibitory crosstalk between ERK and AMPK in the growth and proliferation of cardiac fibroblasts. Biochem Biophys Res Commun 368: 402–407.

Du XL, Edelstein D, Dimmeler S, Ju Q, Sui C, Brownlee M (2001). Hyperglycemia inhibits endothelial nitric oxide synthase activity by posttranslational modification at the Akt site. J Clin Invest 108: 1341–1348.

Esposito DL, Li Y, Cama A, Quon MJ (2001). Tyr(612) and Tyr(632) in human insulin receptor substrate-1 are important for full activation of insulin-stimulated phosphatidylinositol 3-kinase activity and translocation of GLUT4 in adipose cells. Endocrinology 142: 2833–2840.

Fritz T, Krämer DK, Karlsson HK, Galuska D, Engfeldt P, Zierath JR *et al.* (2006). Low-intensity exercise increases skeletal muscle protein expression of PPARδ and UCP3 in type 2 diabetic patients. Diabetes Metab Res Rev 22: 492–498.

Goldin A, Beckman JA, Schmidt AM, Creager MA (2006). Advanced glycation end products: sparking the development of diabetic vascular injury. Circulation 114: 597–605.

Jiménez R, Sánchez M, Zarzuelo MJ, Romero M, Quintela AM, López-Sepúlveda R *et al.* (2010). Endothelium-dependent vasodilator effects of peroxisome proliferator-activated receptor beta agonists via the phosphatidyl-inositol-3 kinase-Akt pathway. J Pharmacol Exp Ther 332: 554–561.

Kilkenny C, Browne W, Cuthill IC, Emerson M, Altman DG (2010). Animal research: Reporting *in vivo* experiments: the ARRIVE guidelines. Br J Pharmacol 160: 1577–1579.

Kim F, Tysseling KA, Rice J, Gallis B, Haji L, Giachelli CM *et al.* (2005). Activation of IKKbeta by glucose is necessary and sufficient to impair insulin signaling and nitric oxide production in endothelial cells. J Mol Cell Cardiol 39: 327–334.

Krämer DK, Al-Khalili L, Perrini S, Skogsberg J, Wretenberg P, Kannisto K *et al.* (2005). Direct activation of glucose transport in primary human myotubes after activation of peroxisome proliferator-activated receptor δ. Diabetes 54: 1157–1163.

Krämer DK, Al-Khalili L, Guigas B, Leng Y, Garcia-Roves PM, Krook A (2007). Role of AMP kinase and PPARdelta in the regulation of lipid and glucose metabolism in human skeletal muscle. J Biol Chem 282: 19313–19320.

Kubota T, Kubota N, Kumagai H, Yamaguchi S, Kozono H, Takahashi T *et al.* (2011). Impaired insulin signaling in endothelial cells reduces insulin-induced glucose uptake by skeletal muscle. Cell Metab 13: 294–307.

Lee CH, Olson P, Evans RM (2003). Minireview: lipid metabolism, metabolic diseases, and peroxisome proliferator-activated receptors. Endocrinology 144: 2201–2207.

Leibowitz MD, Fiévet C, Hennuyer N, Peinado-Onsurbe J, Duez H, Bergera J *et al.* (2000). Activation of PPARδ alters lipid metabolism in db/db mice. FEBS Lett 473: 333–336.

Lim HJ, Lee S, Park JH, Lee KS, Choi HE, Chung KS *et al.* (2009). PPAR delta agonist L-165041 inhibits rat vascular smooth muscle cell proliferation and migration via inhibition of cell cycle. Atherosclerosis 202: 446–454.

Lv ZM, Liu Y, Zhang PJ, Xu J, Jia ZH, Wang R *et al.* (2012). The role of AMPKα in high-glucose-induced dysfunction of cultured rat mesangial cells. Ren Fail 34: 616–621.

McGrath J, Drummond G, McLachlan E, Kilkenny C, Wainwright C (2010). Guidelines for reporting experiments involving animals: the ARRIVE guidelines. Br J Pharmacol 160: 1573–1576.

Miyazaki Y, Mahankali A, Matsuda M, Mahankali S, Hardies J, Cusi K *et al.* (2002). Effect of pioglitazone on abdominal fat distribution and insulin sensitivity in type 2 diabetic patients. J Clin Endocrinol Metab 87: 2784–2791.

Muniyappa R, Quon MJ (2007). Insulin action and insulin resistance in vascular endothelium. Curr Opin Clin Nutr Metab Care 10: 523–530.

Nishikawa T, Edelstein D, Du XL, Yamagishi S, Matsumura T, Kaneda Y *et al.* (2000). Normalizing mitochondrial superoxide production blocks three pathways of hyperglycaemic damage. Nature 404: 787–790.

Oliver WR Jr, Shenk JL, Snaith MR, Russell CS, Plunket KD, Bodkin NL *et al.* (2001). A selective peroxisome proliferator-activated receptor δ agonist promotes reverse cholesterol transport. Proc Natl Acad Sci USA 98: 5306–5311.

Patel MS, Korotchkina LG (2006). Regulation of the pyruvate dehydrogenase complex. Biochem Soc Trans 34: 217–222.

Piqueras L, Sanz MJ, Perretti M, Morcillo E, Norling L, Mitchell JA *et al.* (2009). Activation of PPARbeta/delta inhibits leukocyte recruitment, cell adhesion molecule expression, and chemokine release. J Leukoc Biol 86: 115–122.

Quintela AM, Jiménez R, Gómez-Guzmán M, Zarzuelo MJ, Galindo P, Sánchez M *et al.* (2012). Activation of peroxisome proliferator-activated receptor-β/-δ (PPARβ/δ) prevents endothelial dysfunction in type 1 diabetic rats. Free Radic Biol Med 53: 730–741.

Rains JL, Jain SK (2011). Oxidative stress, insulin signaling, and diabetes. Free Radic Biol Med 50: 567–575.

Reilly SM, Lee CH (2008). PPAR delta as a therapeutic target in metabolic disease. FEBS Lett 582: 26–31.

Reznick RM, Shulman GI (2006). The role of AMP-activated protein kinase in mitochondrial biogenesis. J Physiol 574: 33–39.

Rodríguez-Calvo R, Serrano L, Coll T, Moullan N, Sánchez RM, Merlos M *et al.* (2008). Activation of peroxisome proliferator-activated receptor beta/delta inhibits lipopolysaccharide-induced cytokine production in adipocytes by lowering nuclear factor-kappaB activity via extracellular signal-related kinase 1/2. Diabetes 57: 2149–2157.

Salt IP, Morrow VA, Brandie FM, Connell JM, Petrie JR (2003). High glucose inhibits insulin-stimulated nitric oxide production without reducing endothelial nitric-oxide synthase Ser1177 phosphorylation in human aortic endothelial cells. J Biol Chem 278: 18791–18797.

Saltiel AR, Kahn CR (2001). Insulin signalling and the regulation of glucose and lipid metabolism. Nature 414: 799–806.

Schnyder B, Pittet M, Durand J, Schnyder-Candrian S (2002). Rapid effects of glucose on the insulin signaling of endothelial NO generation and epithelial Na transport. Am J Physiol Endocrinol Metab 282: E87–E94.

Serrano-Marco L, Rodríguez-Calvo R, El Kochairi I, Palomer X, Michalik L, Wahli W *et al*. (2011). Activation of peroxisome proliferator-activated receptor-β/-δ (PPARβ/-δ) ameliorates insulin signaling and reduces SOCS3 levels by inhibiting STAT3 in interleukin-6-stimulated adipocytes. Diabetes 60: 1990–1999.

Taguchi A, White MF (2008). Insulin-like signaling, nutrient homeostasis, and life span. Annu Rev Physiol 70: 191–212.

Tanaka T, Yamamoto J, Iwasaki S, Asaba H, Hamura H, Ikeda Y *et al*. (2003). Activation of peroxisome proliferator-activated receptor δ induces fatty acid β-oxidation in skeletal muscle and attenuates metabolic syndrome. Proc Natl Acad Sci USA 100: 15924–15929.

Terada S, Wicke S, Holloszy JO, Han DH (2006). PPARdelta activator GW-501516 has no acute effect on glucose transport in skeletal muscle. Am J Physiol Endocrinol Metab 290: E607–E611.

Thors B, Halldórsson H, Jónsdóttir G, Thorgeirsson G (2008). Mechanism of thrombin mediated eNOS phosphorylation in endothelial cells is dependent on ATP levels after stimulation. Biochim Biophys Acta 1783: 1893–1902.

Tian XY, Wong WT, Wang NP, Lu Y, Cheang WS, Liu J *et al*. (2012). PPAR delta activation protects endothelial function in diabetic mice. Diabetes 61: 3285–3293.

Tonelli J, Li W, Kishore P, Pajvani UB, Kwon E, Weaver C *et al*. (2004). Mechanisms of early insulin-sensitizing effects of thiazolidinediones in type 2 diabetes. Diabetes 53: 1621–1629.

Vincent MA, Montagnani M, Quon MJ (2003). Molecular and physiologic actions of insulin related to production of nitric oxide in vascular endothelium. Curr Diab Rep 3: 279–288.

Wallis MG, Smith ME, Kolka CM, Zhang L, Richards SM, Rattigan S *et al*. (2005). Acute glucosamine-induced insulin resistance in muscle in vivo is associated with impaired capillary recruitment. Diabetologia 48: 2131–2139.

Wang YX, Lee CH, Tiep S, Yu RT, Ham J, Kang H *et al*. (2003). Peroxisome-proliferator-activated receptor delta activates fat metabolism to prevent obesity. Cell 113: 159–170.

White MF (2003). Insulin signaling in health and disease. Science 302: 1710–1711.

Winzell MS, Wulff EM, Olsen GS, Sauerberg P, Gotfredsen CF, Ahrén B (2010). Improved insulin sensitivity and islet function after PPARδ activation in diabetic db/db mice. Eur J Pharmacol 626: 297–305.

Xu B, Chibber R, Ruggiero D, Kohner E, Ritter J, Ferro A (2003). Impairment of vascular endothelial nitric oxide synthase activity by advanced glycation end products. FASEB J 17: 1289–1291.

Zarzuelo MJ, Jiménez R, Galindo P, Sánchez M, Nieto A, Romero M *et al*. (2011). Antihypertensive effects of peroxisome proliferator-activated receptor-β activation in spontaneously hypertensive rats. Hypertension 58: 733–743.

Supporting information

Additional Supporting Information may be found in the online version of this article at the publisher's web-site:

http://dx.doi.org/10.1111/bph.12646

Figure S1 Insulin-stimulated NO production in physiological (5 mmol L^{-1}) and elevated concentrations of glucose.
Figure S2 Insulin- or A23187-stimulated NO production in HUVECs incubated with physiological concentration of glucose (5 mmol L^{-1}).
Figure S3 Effects of the selective PPARα agonist clofibrate or the PPARγ agonist ciglitazone on impaired insulin-stimulated NO production in high-glucose medium.
Figure S4 Role of AMPK (A, B) and MAPK (C, D) in the protective effects of PPARβ/δ.
Figure S5 Effects of *in vivo* GW0742 treatment in protein expression in aorta from streptozotocin (STZ)-induced diabetic rats.
Figure S6 Role of NO pathway in the effects of GW0742 treatment *in vivo* in aorta from streptozotocin (STZ)-induced diabetic rats.